

# Numerical Study on the Mode I Delamination Toughness of Z-Pinned Laminates

Wenyi Yan<sup>\*1</sup>, Hong-Yuan Liu<sup>1</sup> and Yiu-Wing Mai<sup>1,2</sup>

<sup>1</sup>Centre for Advanced Materials Technology (CAMT), School of Aerospace, Mechanical and Mechatronic Engineering J07, The University of Sydney, Sydney, NSW 2006, Australia

<sup>2</sup>Department of Manufacturing Engineering and Engineering Management (MEEM)  
City University of Hong Kong, 83 Tat Chee Avenue, Kowloon, Hong Kong, China

## Abstract

A finite element (FE) model is developed to investigate mode I delamination toughness of z-pin reinforced composite laminates. The z-pin pull-out process is simulated by the deformation of a set of non-linear springs. A critical crack opening displacement (COD) criterion is used to simulate crack growth in a double-cantilever-beam (DCB) made of z-pinned laminates. The toughness of the structure is quantified by the energy release rate, which is calculated using the contour integral method. The FE model is verified for both unpinned and z-pinned laminates. Predicted loading forces from FE analysis are compared to available test data. Good agreement is achieved. Our numerical results indicate that z-pins can greatly increase the mode I delamination toughness of the composite laminates. The influence of design parameters on the toughness enhancement of z-pinned laminates is also

---

<sup>\*</sup> Corresponding author (Fax: 61 2 9351 7060; Email: w.yan@aeromech.usyd.edu.au).

investigated, which provides important information to optimise and improve the z-pinning technique.

Keywords: B. Fracture toughness; C. Laminates; C. Delamination; C. Computational simulation; Z-pin reinforcement.

## **1. Introduction**

Advanced composite laminates have been extensively used in many structural applications, especially in aerospace engineering due to their strength/weight ratio relative to metallic materials. Traditional fibre composites are manufactured by stacking together a number of plies, in which the fibres are orientated to provide in-plane reinforcement for the composite. A direct consequence of this process is that no fibres are positioned across the laminate thickness. Interlaminar delamination becomes the most common failure mode in composite laminates. A successful solution to this problem is to provide through-thickness reinforcement to the laminated composites because bridging by reinforcing fibres in the laminate thickness provides direct closure tractions to the delamination crack faces. Over the last decade, many techniques have been developed to enhance the strength of the composite laminates in the thickness direction, or z-direction. Among them, a novel approach, so-called z-pinning has been developed by Foster-Miller Inc in the USA [1]. In this technique, short fibres initially contained in foam are inserted into the composite through a combination of

heat and pressure compacting the foam. The z-pinning technique is proven to be a cost effective method to improve the delamination toughness of composite laminates.

Experimentally, the Double-Cantilever-Beam (DCB) is a standard geometry to study mode I delamination toughness of composite laminates. This can be conveniently adopted to evaluate the toughness of z-pinned laminates. Figure 1 schematically illustrates a DCB test for z-pin reinforced composite laminate. Z-pins are inserted in the laminate along the  $z$  direction. The initial crack is created in the laminate mid-plane with length  $a_0$  and the distance of the nearest pin column to the crack tip is  $a_p$ . With increasing external force  $F$  or displacement  $\Delta$  at the loaded ends of the beams, the crack will finally grow along the mid-plane. When the crack reaches the z-pinned zone, the pins will exert closure tractions to close the delaminated crack faces. Thus, a higher external force, compared to an un-pinned crack, is required to maintain the crack growth. That is, the z-pins enhance the delamination toughness of the composite laminate.

Experimental studies to examine the toughness enhancement mechanisms by through-thickness fibres can be found in [2, 3]. To enable a better physical understanding of the effectiveness of z-reinforcement, beam theory has been applied to study theoretically the through-thickness reinforced DCB. Jain and Mai [4] studied the interlaminar mode I fracture reinforced by through-thickness stitching. They developed the first micro-mechanics model to describe fibre pulling out from the through-thickness stitched DCB. The pullout force was then smeared over the reinforced zone in their investigation of the beam deformation. In the

work by Liu and Mai [5], the bridging force of the z-pin is calculated by a fibre pullout model which includes the whole pullout process of the z-pin: elastic deformation before z-pin debonding, elastic deformation and frictional sliding during debonding growth and, finally, frictional sliding. The discrete bridging forces calculated from this pullout model were then applied on the beams. The deformation of the DCB specimen and the pullout displacement were numerically quantified by applying the beam theory.

Instead of focusing on the study of pullout models, the present research tries to establish a FE model to quantify the effect of z-pins on the delamination toughness under mode I loading condition. FE method is robust, which can overcome some limitations of beam theory. Both short-crack and long-crack specimens can be dealt with the FE method. Shear deformation, material orthotropy and geometrical non-linearity can be easily included in a FE investigation by using commercial FE packages. In our FE model, the energy release rate from linear elastic fracture mechanics is applied to quantify the delamination toughness in the present study. Detailed FE simulation process is described Section 2, which includes the simulation of z-pin pullout, the contour integral method to calculate the energy release rate and the application of the critical COD criterion. This established FE model is then verified by benchmarking predicted numerical results against theoretical solutions for the unpinned laminates. Numerical results of unpinned and z-pinned laminated composites are given in Section 3. The predicted forces at the loaded ends of the DCB during delamination growth are compared with available experimental results.

## 2. Theoretical Approach

### 2.1 Toughness analysis

According to linear elastic fracture mechanics theory, the toughness of a material or structure can be quantified by the energy release rate,  $G_a$ , which is defined as ([6])

$$G_a = \frac{1}{w} \left( \frac{dU_e}{da} - \frac{dU_s}{da} \right), \quad (1)$$

where  $w$  is width of the crack front equal to the DCB width,  $a$  is crack length,  $U_e$  is external work performed and  $U_s$  is stored elastic energy. The energy release rate  $G_a$  represents the energy available for the creation of a unit new crack area.

For unpinned DCB specimens, the dissipated energy is completely consumed by the surface energy of the newly created crack surface, which is denoted by  $G_c$ . During crack growth,  $G_c$  must be equal to the composite's intrinsic toughness,  $G_{IC}$ . Hence,

$$G_a = G_c = G_{IC}. \quad (2)$$

For z-pin reinforced DCB specimens, the dissipated energy includes not only the crack surface energy but also the energy dissipated during the z-pin pullout process, which includes the elastic energy of the pins, the surface debonding energy between pins and the composite and the friction energy consumed during pullout. Therefore, the total energy release rate of a z-pinned DCB specimen,  $G_a$ , consists of two parts: the energy release rate for the new crack

surface,  $G_c$ , and the energy release rate due to z-pin pullout,  $G_p$ , which depends on the extent of delamination. That is,

$$G_a = G_c + G_p(\Delta a) \quad (3)$$

and  $G_c = G_{IC}$ . The delamination toughness of z-pinned laminates can be completely described by the total energy release rate,  $G_a$ , which is commonly called the crack-resistance  $G_R$ . The FE method is applied to analyse  $G_a$  or  $G_R$  of z-pin reinforced DCB specimens.

## 2.2 Pullout model and pullout simulation

Z-pin pullout from laminate composites is a very complex process. The whole pullout process normally consists of three stages. In the first stage, the interface between the z-pin and the laminate is perfectly bonded. The bridging force is caused by the elastic deformation of the z-pin. With increasing load, the interfacial shear stress between z-pin and laminate exceeds the interfacial shear strength. Debonding starts and propagates. In this stage, the bridging force of the z-pin is caused by both elastic deformation (in bonded region) and interfacial friction (in debonded region). After the interface has fully debonded, the z-pin is pulled out from the laminate. The bridging force at the final stage is completely controlled by friction. Detailed discussion and analysis of the pin-pullout process can be found in [7]. For the purpose of our current study, we consider a simple pullout model. This model is represented by the function between the bridging force,  $P$ , and the pullout displacement,  $\delta$ . A bi-linear function is adopted to describe their relationship, which is

$$P = \begin{cases} \frac{P_a}{\delta_a} \delta, & 0 \leq \delta \leq \delta_a \\ P_a - \frac{P_a}{h - \delta_a} (\delta - \delta_a), & \delta_a \leq \delta \leq h \end{cases} \quad (4)$$

This function is shown in Fig. 2, which clearly indicates that this pullout model is completely determined by the peak bridging force,  $P_a$ , its corresponding pullout displacement,  $\delta_a$ , and the ultimate pull-out displacement,  $h$ , equal to half-thickness of the DCB. The bridging force is zero when the pin completely pulls out from the composite, that is, when  $\delta = h$ .

This pullout model can also be applied to describe the case where the pin ruptures before being completely pulled out, which was discussed by Jain and Mai [4]. This happens when the pullout force is larger than the rupture force of the pin. This becomes possible if the bonding between the pin and the laminate is strong enough. In this special case, the pullout force drops to zero immediately after it reaches the maximum value  $P_a$ .

For simplicity, the pullout process of a z-pin from the composite laminate is not explicitly simulated in our FE analysis. Instead, the pin effect is simulated by distributed springs along the thickness of the beam at the same location, which is schematically shown in Fig. 3. Note that a section of the z-pinned laminate with a pin pulling-out is given in Fig. 3(a) and its FE model in Fig. 3(b). Several identical non-linear springs are arranged on the FE nodes, which are highlighted by black dots in Fig. 3(b).

The functional form of Eq. 4 is applied to describe the properties of the non-linear springs. But now, the peak bridging force per unit width,  $p_s$ , of a non-linear spring in plane stress is

used to simulate the pin pullout process. This is determined in our FE model by

$$p_s = \frac{P_a n_r}{w n_s}, \quad (5)$$

where  $n_r$  is the number of rows of pins arranged along the beam width, i.e., the y-direction in Fig. 1. The number of identical springs in one column used to represent a column of pins is denoted by  $n_s$ . Our trial calculations indicate that the results for  $n_s$  from 4 to 9 are the same. Hence,  $n_s$  is chosen as 8 throughout all the FE calculations.

## 2.3 Contour integral

The energy release rate is calculated by the contour integral method. According to linear elastic fracture mechanics (see [6]), the energy release rate,  $G_a$ , is equal to a contour integral with the integrating path starting from the lower crack surface and ending at the upper crack surface, i.e.,

$$G_a = \int_{\Gamma} W_s dz - (T_x \frac{du_x}{dx} + T_z \frac{du_z}{dx}) dS, \quad (6)$$

where  $W_s$  is the strain energy density of the composite,  $T_x$  and  $T_z$  are components of the traction vector at the section  $dS$  of the contour  $\Gamma$ .  $u_x$  and  $u_z$  are the displacement components, see Fig. 4.

Two contours,  $\Gamma_1$  and  $\Gamma_2$ , are shown in Fig. 4. Contour  $\Gamma_1$  includes only the composite around the crack-tip without the springs, i.e., z-pins. The calculated energy release rate  $G_a$  based on contour  $\Gamma_1$  corresponds to  $G_c$ , which is equal to the intrinsic toughness of the unpinned

composite. Thus,  $G_a = G_c = G_{IC}$ . Contour  $\Gamma_2$  includes all the springs, that is, all the effects of the z-pins. The calculated energy release rate, based on this contour,  $G_a$ , now represents the total energy release rate, which includes the energy dissipation due to the creation of new crack surfaces  $G_a$  and the energy dissipation due to the z-pins  $G_p$ . As described Section 2.1,  $G_a$  is the same as the crack-resistance  $G_R$  of the z-pinned DCB.

The FE package ABAQUS adopts a domain integral method to numerically calculate the contour integral based on the divergence theorem. This method has been proved to be quite effective in the sense that accurate contour integral estimates are usually obtained even with quite coarse meshes because the integral is taken over a domain of elements surrounding the crack front. Errors in local solution parameters have less effect on the domain integrated value, i.e., the energy release rate (see, ABAQUS [8]). Therefore, it is not necessary to simulate the stress singularity near the crack-tip. Ordinary 4-node bi-linear plane stress elements are used in our FE analyses. Fig. 3(b) shows part of the FE meshes. In total, there are about 13,700 elements used in the FE model. It takes about 16 h in a Compaq ES45 supercomputer with one CPU to finish a crack growth simulation.

## 2.4 The critical COD criterion

According to fracture theory, the energy release rate criterion is equivalent to the crack opening displacement criterion, see Anderson [9]. Sih et al [10] studied the general crack

problem in orthotropic materials. The relation between the energy release rate,  $G_a$ , and the COD is (see, also Suo [11] and Poursartip et al. [12])

$$\text{COD} = 4(2)^{1/4} \frac{(a_{11}a_{22})^{1/4}}{\sqrt{\pi}} \left( \frac{2a_{12} + a_{66}}{2a_{11}} + \sqrt{\frac{a_{22}}{a_{11}}} \right)^{1/4} \sqrt{G_a} \sqrt{r}, \quad (7)$$

where  $a_{11}$ ,  $a_{22}$ ,  $a_{12}$  and  $a_{66}$  are determined by material elastic constants. In the case of plane stress studied here, they are ([13])

$$\begin{aligned} a_{11} &= \frac{1}{E_1}, & a_{22} &= \frac{1}{E_2}, \\ a_{12} &= -\frac{\nu_{21}}{E_2} = -\frac{\nu_{12}}{E_1}, & a_{66} &= \frac{1}{G_{12}}. \end{aligned} \quad (8)$$

The  $r$  in Eq (7) represents the distance from the crack-tip, which is illustrated in Fig. 4.

The finite element package ABAQUS provides the critical COD fracture criterion to simulate crack growth, which is applied in the present study. In this case, the crack grows by releasing the node in front of the crack-tip when the COD at a specified distance behind the crack-tip reaches a critical value. In our study, the specified distance is determined by several trial tests based on the rule that the calculated energy release rate should be the same as the critical value used to determine the critical COD for the unpinned DCB.

Recall Fig. 3, in order to construct the kind of contours  $\Gamma_2$  to include all the springs, as that shown in Fig. 4, the springs are not arranged on the top nodes of the beam. Also, because the critical COD criterion is applied to simulate crack growth, it is crucial that the concentrated force from the springs should not strongly affect the local crack-tip displacements. Hence, the springs are not arranged on the bottom nodes immediately close to the crack surface. Thus,

contours like  $\Gamma_1$  can be constructed to exclude all the springs. This arrangement for the springs partly reflects the reality because bonding at both ends of a pin is normally not as good as that in the middle, which originates from the z-pin insertion process and the z-pin bending effect. Furthermore, because the energy release rate is used to quantify the toughness of the structure, the local errors due to the arrangement of the springs is expected to have little effect on the contour integral of the energy release rate.

## 2.5 Material and geometry data

DCB tests had been carried out to study mode I delamination behavior of z-pinned composite laminates by Cartie and Partridge [14]. The material constants and geometrical parameters used in our FE calculations are based on their test results, which are summarized in Tables 1 and 2 below.

In Table 1,  $E_1$  and  $E_2$  are Young's moduli in  $x$ - and  $z$ -direction, respectively.  $\nu_{12}$  is Poisson coefficient, which characterizes compression in  $z$ -direction due to tension along  $x$ -direction.  $\mu_{12}$  is shear modulus for planes parallel to the coordinates  $xOz$ . The values of the parameters to describe the DCB and z-pinning are listed in Table 2.

Here  $h$  is half-thickness,  $w$  width and  $L$  total length of the DCB. The parameter  $a_o$  is the initial length of the crack and  $a_p$  is the distance from the crack-tip to the closest pins. As shown in Fig. 2,  $P_a$  is the peak force during a single pin pullout and  $\delta_a$  is the corresponding

pullout displacement.  $n_c$  is number of columns of pins arranged in  $x$ -direction and  $n_r$  is number of rows of pins arranged in  $y$ -direction.  $d_c$  represents the column spacing between adjacent z-pin columns.

## 2.6 Model verification

For unpinned DCB, there are no z-pins to improve delamination toughness of the composite laminate. The energy release is only consumed in creation of new crack surfaces. That is,  $G_p = 0$ . Thus, from Eq. 3, we have

$$G_a = G_c = G_{IC}. \quad (9)$$

Theoretically, the calculated energy release rate,  $G_a$ , from the FE analysis using the contour integral method should be the same value as the critical energy release rate  $G_{IC}$  used to calculate the critical COD during crack growth. Based on this consideration, FE analysis is first carried out to simulate crack growth in the unpinned DCB. Figure 5 shows the variation of  $G_a$  with crack growth,  $\Delta a$ , for different inputted critical energy release rate,  $G_{IC}$ . It clearly demonstrates that the energy release rates are the same during crack growth in all the cases. All the curves indicate very good agreement between the calculated energy release rate and the inputted critical energy release rate is achieved in each case.

For un-pinned DCB, the reaction force at the loaded ends should decrease gradually during crack growth. This is confirmed in Fig. 6, in which the solid line represents the numerically calculated reaction force plotted against crack growth. Here,  $G_{IC}$  is assumed  $265 \text{ J/m}^2$  and the

beam width,  $w$ , is 20 mm. Because the initial crack length is much larger than the height of the DCB, the analytic solution from conventional beam theory is a good approximation for this case although it neglects the effect of material orthotropy. Thus, we have (see [9])

$$F = \left( \frac{w^2 h^3 E_{11} G_{IC}}{12a^2} \right)^{1/2}. \quad (10)$$

The chained line in Fig. 6 represents the analytic solution from Eq. (10). The results from the beam theory are no more than 4% higher than the FE results.

Including the effect of material orthotropy, Suo et al [15] proposed a more accurate solution for the energy release rate of un-pinned DCB specimens (also see [16]). Their solution is obtained using finite elements, together with several analytic considerations and the error is within 1%. Based on the solution of Suo et al [15], in the case of plane stress, the reaction force is determined by

$$F = \left( \frac{w^2 h^3 E_{11} G_{IC}}{12a^2 (1 + Y\lambda^{-1/4} h/a)^2} \right)^{1/2}, \quad (11)$$

where  $\lambda = a_{11} / a_{22}$ . The dimensionless factor  $Y$  is approximated by

$$Y(\rho) = 0.677 + 0.149(\rho - 1) - 0.013(\rho - 1)^2 \quad (12)$$

with  $\rho = (a_{12} + 0.5a_{66}) / (a_{11}a_{22})^{1/2}$ . Inserting values of material parameters, results from Eq. (11) are also shown in Fig. 6 by the dotted line, which clearly shows that our FE results (solid line) agree very well with those of Suo et al [15]. Thus, our FE model based on the critical COD criterion and the energy release rate concept can be used to study the delamination toughness of z-pinned laminates. The results shown in Section 2.7 further confirm our FE model.

## 2.7 Dimensional analysis

Crack growth in z-pinned DCB is fairly complex. Too many parameters contribute to the failure process. Hence, to study the major effects of some of these parameters, dimensional analysis is adopted. Generally, given a material's elastic property, the functional dependency of the crack-resistance,  $G_R$ , on the independent parameters is

$$G_R = g_1(F, \Delta a, a_0, a_p, w, h, G_{IC}, P_a, \delta_a, n_c, d_c, n_r, d_r), \quad (13a)$$

where  $d_r$  is spacing between adjacent z-pin rows. The reaction force  $F$  at the loaded ends is a physical quantity similar to  $G_R$ . Therefore, during crack growth,  $G_R$  actually depends on:

$$G_R = g_2(\Delta a, a_0, a_p, w, h, G_{IC}, P_a, \delta_a, n_c, d_c, n_r, d_r). \quad (13b)$$

Due to our plane stress assumption, the effect of row spacing,  $d_r$ , can be ignored. According to Eq (5), the peak force in the springs of our model,  $p_s$ , is determined by the product of the peak force of the single pin pullout model,  $P_a$ , and number of z-pins in a row,  $n_r$ . Therefore, in the parametrical study, we can just focus on the effect of  $P_a$  while fixing the number of z-pins in a row,  $n_r$ , which is chosen as 5 according to Cartie and Partridge [14]. Furthermore, the initial crack length  $a_0$  is determined by standard DCB tests, which is 50 mm in our simulations. The effect of the distance of the z-pinned zone from the initial crack tip,  $a_p$ , can be implicitly reflected in the effect of the crack growth  $\Delta a$ . Hence,  $a_p$  is also fixed as 5 mm in our analysis. After these considerations, the function of the crack-resistance of the DCB is simplified as:

$$G_R = g_3(\Delta a, h, G_{IC}, P_a, \delta_a, n_c, d_c) \quad (13c)$$

According to the dimensional theory, see Anderson [9], we have the follow dimensionless function

$$\frac{G_R}{G_{IC}} = g_4\left(\frac{\Delta a}{h}, \frac{\delta_a}{h}, \frac{P_a}{G_{IC}h}, \frac{d_c}{h}, n_c\right). \quad (14)$$

Thus, the normalized crack-resistance or “apparent” crack toughness of the z-pinned DCB,  $G_R/G_{IC}$ , is completely determined by the dimensionless crack advance,  $\Delta a/h$ , normalized location of peak force in the pullout model,  $\delta_a/h$ , normalized peak force in pullout model,  $P_a/(G_{IC}h)$ , normalized pin column spacing,  $d_c/h$ , and number of columns of pins,  $n_c$ . Based on Eq (14), the effects of these parameters on the delamination toughness of DCB are studied in Section 3.

### 3. Results and Discussion

#### 3.1 Comparison with experimental data

Whilst DCB tests were carried out on mode I delamination of z-pinned composite laminate ([14]), there has been no reliable test data to-date for z-pin pullout to our knowledge. Hence, different peak forces of the pullout model,  $P_a$ , were selected in our FE simulations. For  $P_a=15$  N, the FE output of the reaction force of the DCB *versus* opening displacement at the load-points is shown by the solid line in Fig. 7. It shows that the force increases linearly with opening displacement at the initial stage, which corresponds to the linear deformation of the DCB before crack growth. The force drops immediately after the crack has started to propagate. If there were no z-pins, the force would continue to decrease as shown in Fig. 6.

However, due to the closure tractions exerted by the z-pins, the applied force increases gradually over a wide range of crack growth. The maximum value reaches ~80 N, which is much larger than the maximum force of the unpinned specimen. This means that the delamination toughness of the DCB has been greatly improved by the z-pins. At the final stage, the load drops again because all the pins have been pulled out. The black dots are the experimentally measured data from [14], and compared to our FE results using  $P_a=15$  N, very good agreement is obtained.

### 3.2 Z-pin enhanced toughness

As described above, the energy release rate is a suitable parameter to quantify the toughness of a structure. Here, the energy release rate *versus* crack growth, or  $G_R$ -curve, obtained from our FE analysis is calculated using a  $\Gamma_2$  type contour in Fig. 4 and represented in Fig. 8 by the solid line. The dotted line is the FE result of the energy release rate for the unpinned sample, which is constant during crack growth and is equal to  $G_{IC} = 265$  J/m<sup>2</sup>. The dashed line is the energy release rate,  $G_c$ , derived from the z-pinned DCB based on a  $\Gamma_1$  type contour in Fig. 4.

As discussed above,  $G_c$  should represent the energy release rate due solely to the creation of new crack surfaces during delamination crack growth, that is,  $G_c=G_{IC}$ . Fig. 8 clearly confirms this prediction. This fact further verifies that our FE model based on a critical COD criterion can be applied to effectively simulate mode I delamination in a z-pinned composite laminate. The results from our simulations are hence accurate.

Comparing the solid and dotted lines in Fig. 8, it is shown that the crack-resistance  $G_R$ -curve of the z-pinned laminate is overall much larger than the unpinned laminate except at initial crack growth, where the z-pins have not yet started to function. The maximum  $G_R$  is  $\sim 1900$  J/m<sup>2</sup>, which is  $\sim 7$  times the unpinned DCB. Hence, z-pinning is a very effective technique to improve the mode I delamination toughness of composite laminates.

### 3.3 Parametric study

To understand the contribution of the parameters discussed in Section 2.6 on z-pin enhanced toughness of DCB, a parametrical study is quantitatively carried out. The effect of the pullout model is studied first. Fig. 9 shows the influence of the normalized pullout model parameter,  $\delta_a/h$ , on the normalized energy release rate,  $G_R/G_{IC}$ , during crack growth. In all the three cases for  $\delta_a/h$  from 0.0667 to 0.133 and 0.267, the other parameters are fixed at  $n_c = 8$ ,  $\delta_c/h = 2.33$  and  $P_a/G_{IC}h = 61.9$ . Fig. 9 shows that the crack-resistance  $G_R$  increases in all three cases due to z-pin reinforcement. However, the difference is small, especially at the plateau region there is no difference. Thus, the effect of the pullout parameter  $\delta_a$  on toughness enhancement is not significant.

The effect of the normalized pullout model parameter,  $P_a/G_{IC}h$ , is shown in Fig. 10. It can be seen that the total energy release rate or crack-resistance increases as the peak pullout force,  $P_a$ , increases. For  $P_a/G_{IC}h = 37.7$ , the maximum normalized crack-resistance,  $G_R/G_{IC}$ , is about

7 but this becomes  $>13$  for  $P_a/G_{ICh}=75.7$ . The contribution of the z-pins on the enhanced toughness is a manifestation of the work dissipated in pulling out the pins. That is, the work area under the curve of the pullout force  $P$  versus pullout displacement  $\delta$  in Fig. 2. The parameter  $\delta_a$  represents the pullout displacement at maximum pullout force,  $P_a$ . Thus, by increasing  $P_a$  the area in Fig. 2 and hence the z-pin pullout work is also increased. This in turn improves the delamination toughness of a z-pinned structure. Conversely, changing the value of  $\delta_a$  alone without varying  $P_a$  cannot change the z-pin pullout work. Hence, the effect of  $\delta_a$  on  $G_R$  should be small as confirmed by Fig. 9. These conclusions are consistent with the study on cohesive failure (see [17]). Practically, higher pullout peak force  $P_a$  can be achieved by improving the z-pining technique to gain stronger bonding between pins and laminate.

Figure 11 shows the influence of the number of z-pin columns on the energy release rate of z-pinned laminates. Here six cases are considered for  $n_c = 1$  to 8. The number of z-pin columns represents the size of the z-pinned zone in the crack growth direction for a given column spacing,  $d_c$ . Therefore, it is not surprised to see that the enhanced toughness  $G_R/G_{IC}$  covers a longer delaminated distance for higher number of z-pin columns. Fig. 11 also shows that the maximum crack-resistance  $G_R$  increases rapidly from  $n_c = 1$  to 4. This observation indicates that interaction between pin columns can also enhance the delamination toughness of the composite laminate. With  $n_c$  increasing continuously from 4 to 8, this effect becomes less efficient. For example,  $G_R/G_{IC}$  are almost identical for  $n_c = 6$  and 8. Hence, it is expected that further increasing  $n_c$  beyond 8 would not lead to any improvement in  $G_R/G_{IC}$ . In sum, there is a limit to the enhanced toughness by simply increasing the number of the z-pin columns.

However, Fig. 11 also indicates that a steady toughening state can be reached when the number of the z-pin columns is over 8.

The influence of the normalized column spacing,  $d_c/h$ , on the normalized energy release rate,  $G_R/G_{IC}$ , is shown in Fig. 12. By keeping the same number of z-pin columns, the delamination toughness is shown to increase with decreasing column spacing. This confirms the interactive effect between z-pin columns. That is, smaller column spacing provides stronger interaction between z-pin columns. This prediction is consistent with experimental results. Cartie and Patridge [14] found in their tests that increasing the z-pin density by reducing the spacing distance greatly increased the mode I delamination toughness of DCB specimens. However, it must be remembered that the present results are obtained based on a single pin pullout model. Detailed experimental and theoretical study should be carried out to determine the limits of the application of the single pin pullout model in multi-pin reinforced laminates.

## 4. Conclusions

A FE analysis model is developed to study the mode I delamination toughness of z-pinned composite laminates. The effect of z-pins is simulated by suitably arranging the non-linear springs. A critical COD criterion is used to simulate crack growth in a DCB specimen, made of z-pinned laminates. The delamination toughness is quantified by the energy release rate, which is calculated by using the contour integral method. The FE model is verified for both un-pinned and z-pinned laminates. The predicted force as a function of opening displacement

at the loaded ends of the DCB sample agrees well with available experimental data. Our numerical results indicate that z-pins can greatly increase mode I delamination toughness of composite laminates. Parametric study shows that increasing the pullout peak force through improving z-pinning technique can greatly improve the delamination toughness of z-pinned laminates. Furthermore, increasing the number of z-pin columns dramatically enhances the peak crack toughness, but this beneficial effect saturates when the column number reaches a certain value. The column spacing is also a sensitive parameter that affects the delamination toughness. Our results show that by reducing the distance between adjacent z-pin columns the peak toughness is increased.

## **Acknowledgements**

We wish to thank the HKSAR Research Grants Council (CERG Project # 9040613) for the continuing support of our z-pinning project. The supports of the Australian Research Council to WY (Research Associate), H-YL (Research Fellow) and Y-WM (Federation Fellow) are also much appreciated. Some of the calculations were carried out at the National Facility of the Australian Partnership for Advanced Computing through an award under the Merit Allocation Scheme to WY.

## References

1. Freitas G, Magee C, Dardzinski P, Fusco T. Fiber insertion process for improved damage tolerance in aircraft laminates. *J Adv Mater* 1994; 25(4): 36-43.
2. Rugg KL, Cox BN, Massabo R. 2002. Mixed mode delamination of polymer laminates reinforced through the thickness by z-fibres. *Composites Part A* 2002; 33: 177-190.
3. Rugg KL, Cox BN, Ward KE, Sherrick GO. Damage mechanisms for angled through-thickness rod reinforcement in carbon-epoxy laminates. *Composites Part A* 1998; 29:1603-1613.
4. Jain LK, Mai Y-W. On the effect of stitching on mode I delamination toughness of laminated composites. *Comp Sci and Tech* 1994; (51):331-345.
5. Liu H-Y, Mai Y-W. Effects of z-pin reinforcement on interlaminar mode I delamination. In: *Proceedings of the 13<sup>th</sup> international conference on composite materials, ICCM13, Beijing, 25<sup>th</sup>-29<sup>th</sup> June, 2001.*
6. Williams JG. 1989. Fracture mechanics of anisotropic materials. In: Friedrich K editor. *Application of fracture mechanics to composite materials.* Amsterdam: Elsevier, 1989.
7. Liu H-Y, Zhang X, Mai Y-W, Diao, X-X. On steady-state fibre pull-out part II: Computer simulation. *Comp Sci Tech* 1999; (59):2191-2199.
8. ABAQUS 2001 Version 6.2. Providence, RI: HKS Inc.
9. Anderson TL. *Fracture mechanics: Fundamentals and applications.* Second Edition, Boca Raton: CRC Press, 1995.

10. Sih GC, Paris PC, Irwin GR. On cracks in rectilinearly anisotropic bodies. *Int J Fract Mech* 1965; 1(1):189-203.
11. Suo Z. Delamination specimens for orthotropic materials. *ASME J Appl Mech* 1990; (57):627-634.
12. Poursartip A, Gambone A, Ferguson S, Fernlund G. 1998. In-situ SEM measurements of crack tip displacements in composite laminates to determine local G in mode I and II. *Eng Frac Mech* 1998; 60:173-185.
13. Lekhnitskii SG. *Theory of elasticity of an anisotropic elastic body*. San Francisco: Holden-Day, Inc. 1963.
14. Cartie DDR, Partridge IK. Delamination Behaviour of Z-pinned Laminates. In: *Proceedings of the 12<sup>th</sup> international conference on composite materials, ICCM12, Paris 5<sup>th</sup>-9<sup>th</sup> July, 1999*.
15. Suo Z, Bao G, Fan B, Wang, TZ. Orthotropy rescaling and implications for fracture in composites. *Int J Solids Struct* 1991; 28:235-248.
16. Hutchinson JW, Suo Z. Mixed mode cracking in layered materials. *Advances in Applied Mechanics* 1991; 29:63-191.
17. Williams JG, Hadavinia H. Analytical solutions for cohesive zone models. *J Mech Phys Solids* 2002; 50:809-825.

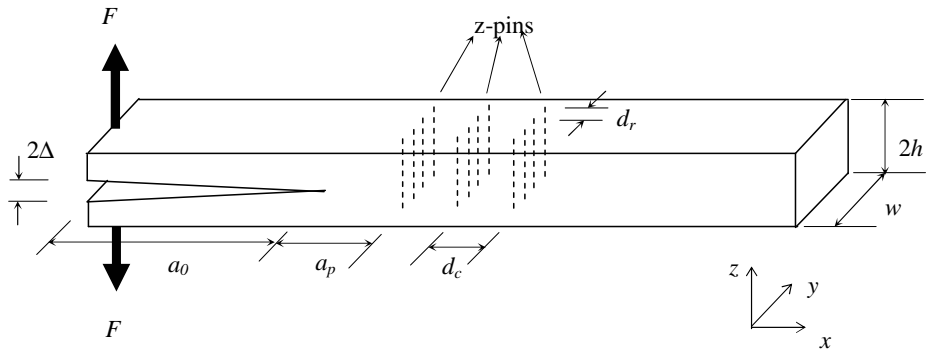


Figure 1. Schematic of a Double-Cantilever-Beam (DCB) test for z-pinned composite laminate.

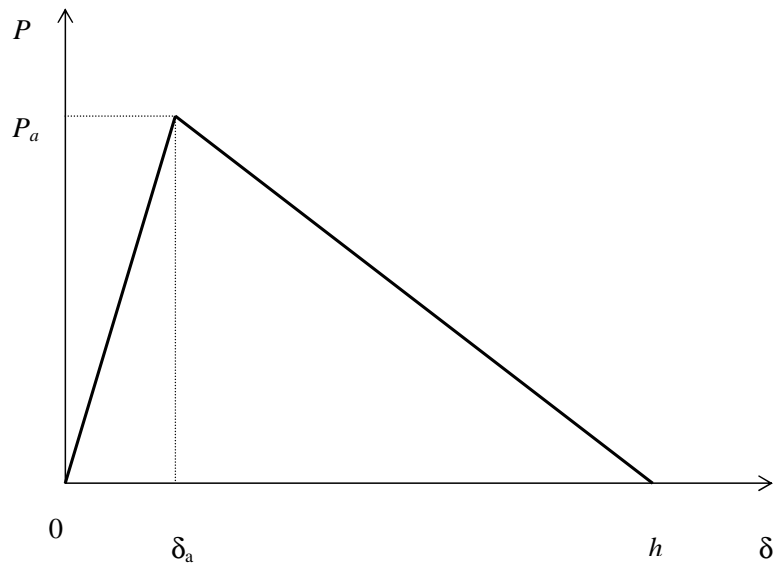


Figure 2. Illustration of the z-pin pullout model used in this study.

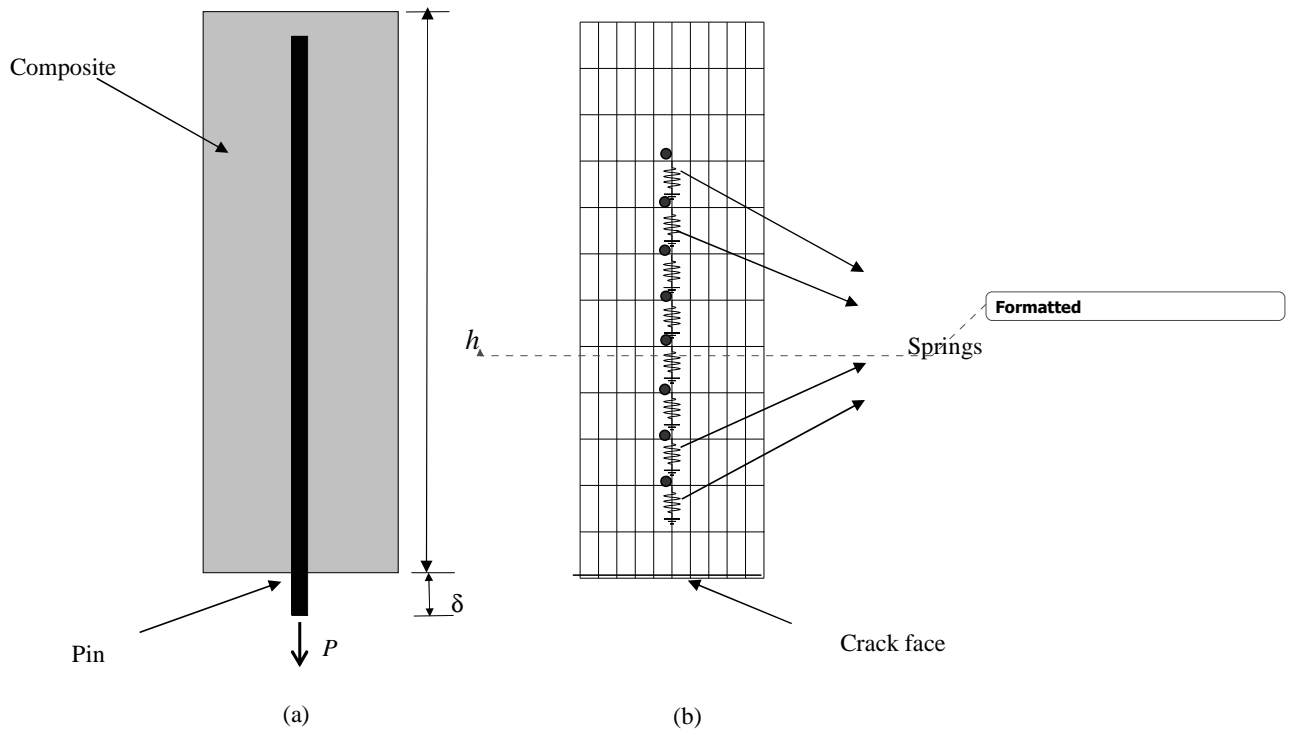


Figure 3. Schematically illustrating FE simulation of the effect of z-pin by distributed nonlinear springs in FE model: (a). a section of z-pinned composite; (b). FE model for this section with distributed springs.

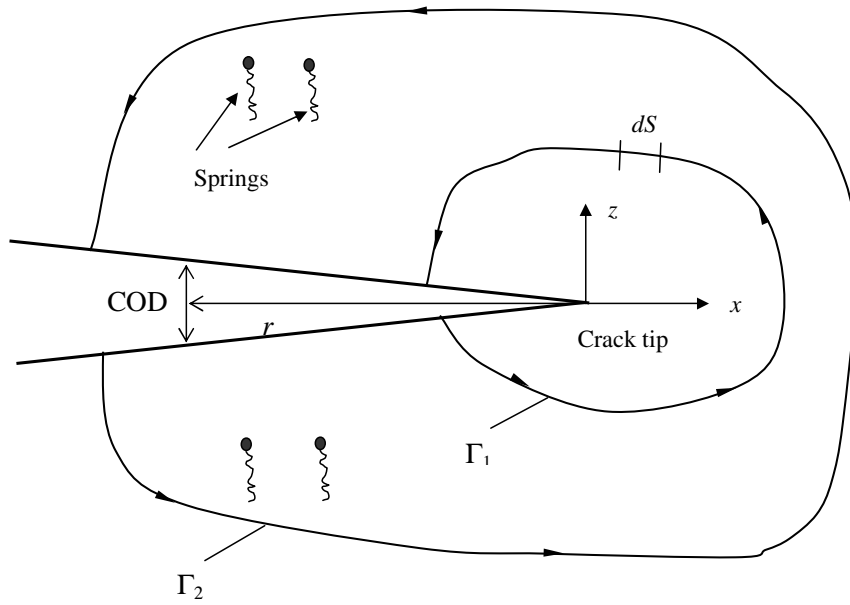


Figure 4. Integral contours for calculating energy release rates:  $\Gamma_1$ : contour excluding springs (z-pins);  $\Gamma_2$ : contour including all the springs (z-pins).

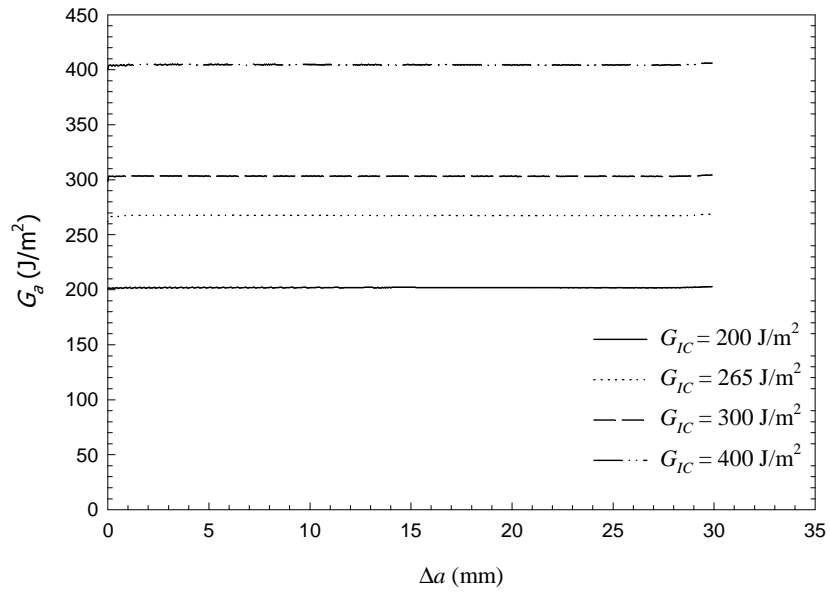


Figure 5. Calculated energy release rate of an un-pinned DCB as a function of crack growth for different critical energy release rates.

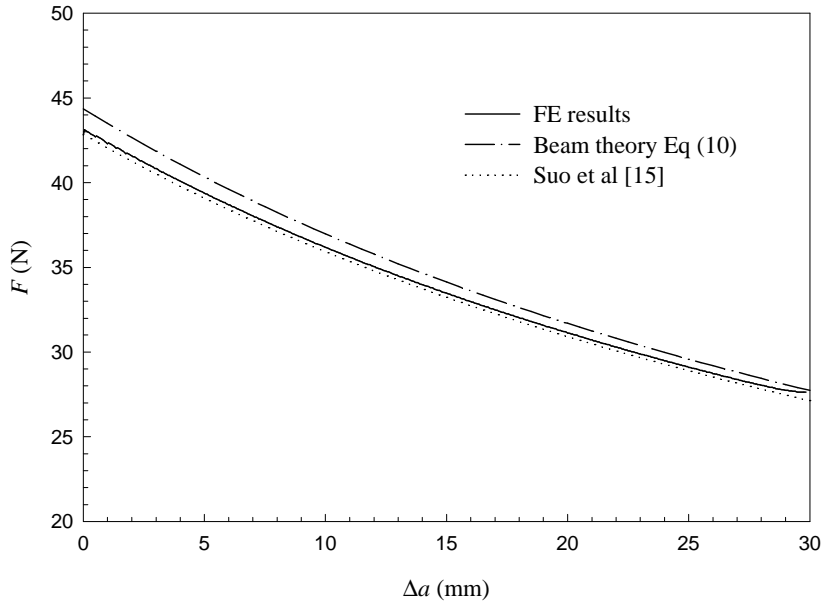


Figure 6. The reaction force at the loaded ends,  $F$ , as a function of crack growth,  $\Delta a$ , for an un-pinned DCB with  $G_{IC}=265 \text{ J/m}^2$  and  $w=20 \text{ mm}$ .

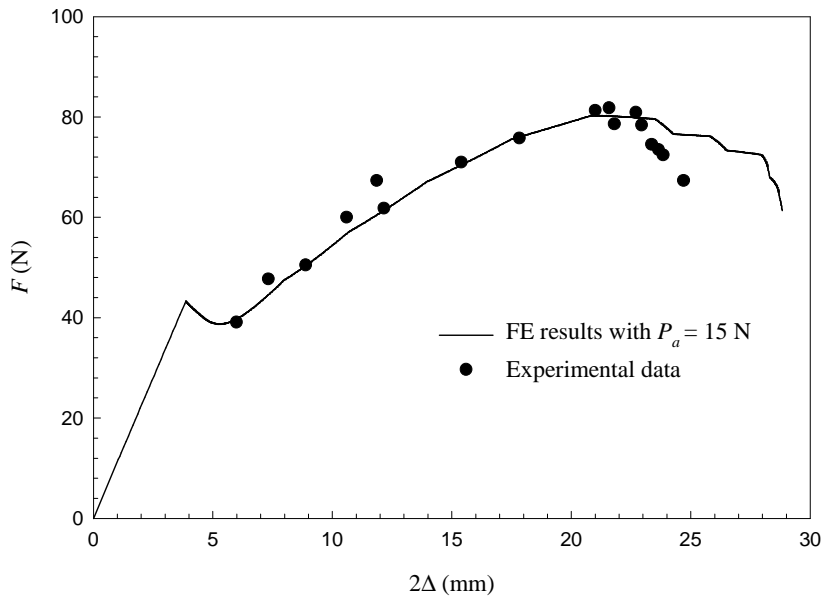


Figure 7. A plot of the applied force and opening displacement at the loaded ends of a DCB during delamination growth.

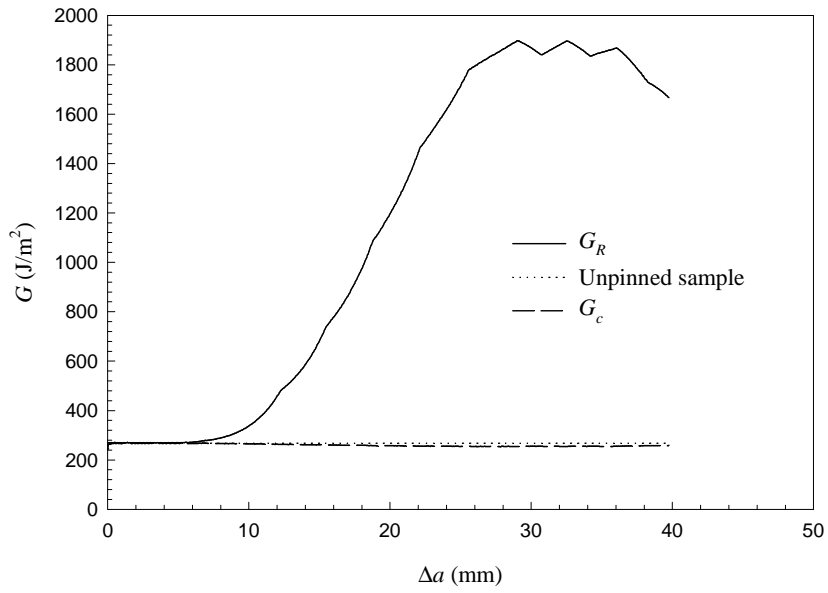


Figure 8. Calculated energy release rates as a function of crack growth with  $G_{IC} = 265 \text{ J/m}^2$

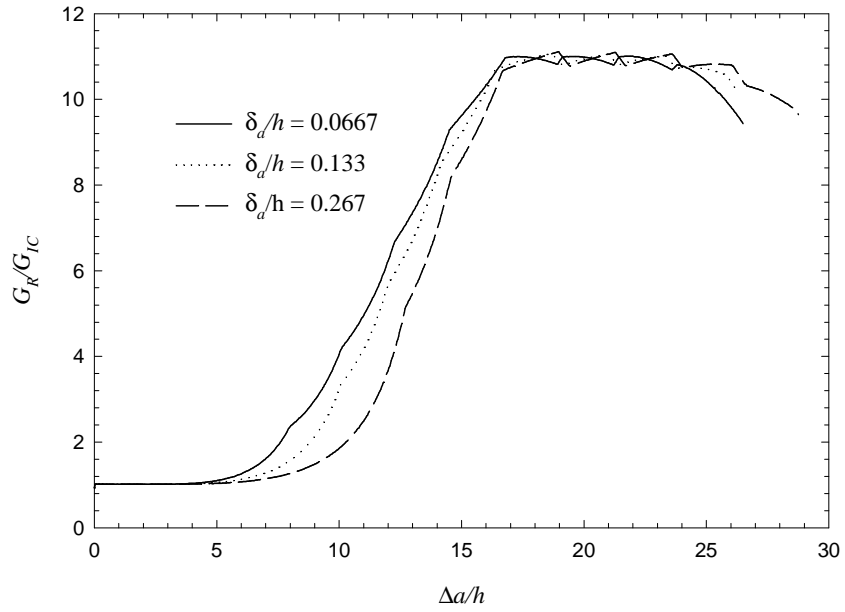


Figure 9. Influence of normalized pullout model parameter,  $\delta_d/h$ , on normalized delamination toughness,  $G_R/G_{IC}$ , during crack growth with  $n_c = 8$ ,  $P_d/G_{IC}h = 61.9$  and  $d_c/h = 2.33$ .

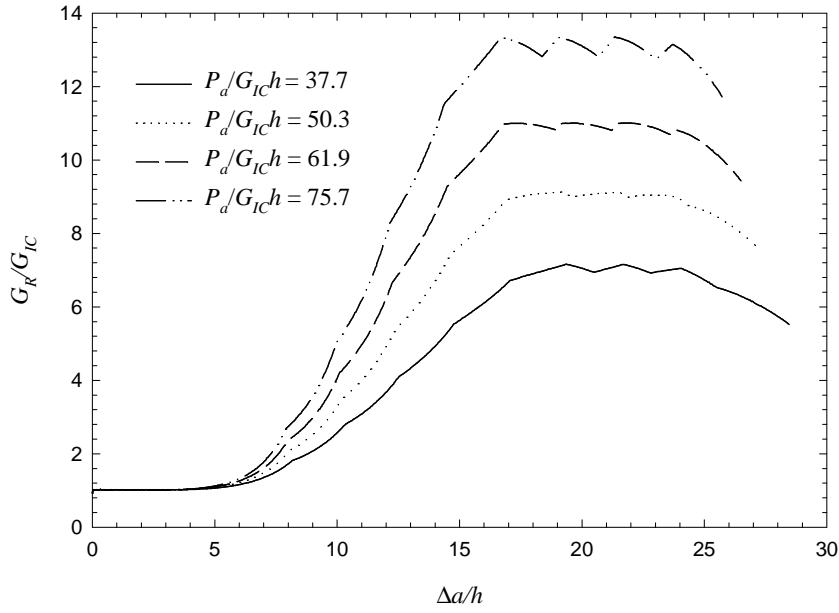


Figure 10. Influence of normalized pullout model parameter,  $P_d/G_{IC}h$ , on normalized delamination toughness,  $G_R/G_{IC}$ , during crack growth with  $n_c = 8$ ,  $\delta_d/h = 0.0667$  and  $d_c/h = 2.33$ .

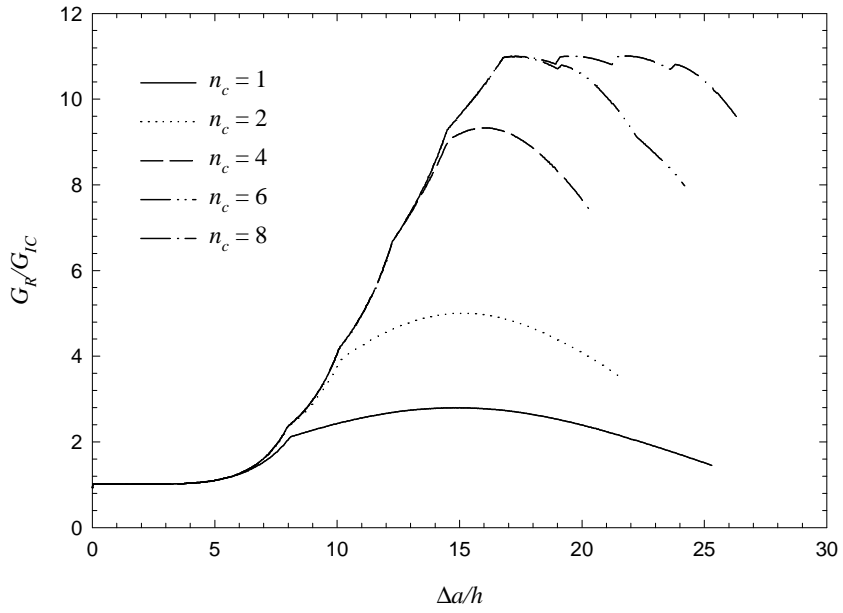


Figure 11. Influence of number of z-pin columns,  $n_c$  on normalized delamination toughness,  $G_R/G_{IC}$ , during crack growth with  $P_d/G_{ICh} = 61.9$ ,  $\delta_d/h = 0.0667$  and  $d_c/h = 2.33$ .

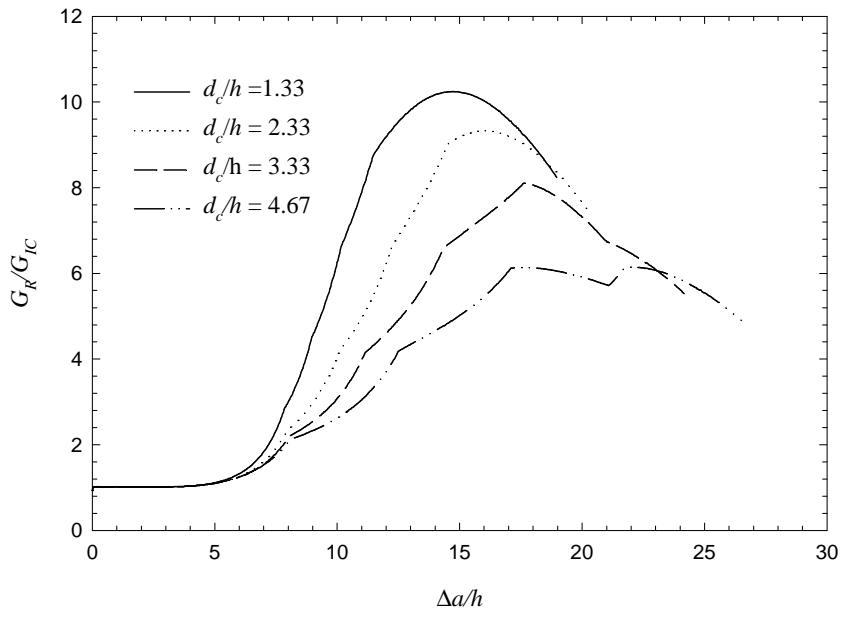


Figure 12. Influence of normalized column spacing,  $d_c/h$ , on normalized delamination toughness,  $G_R/G_{IC}$ , during crack growth with  $P_d/G_{IC}h = 61.9$ ,  $\delta_d/h = 0.0667$  and  $n_c = 4$ .

Table 1. The material constants of the composite laminate.

$E_1$ (GPa)	$E_2$ (GPa)	$\nu_{12}$	$\mu_{12}$ (GPa)
165	11	0.3	38

Table 2. Values of parameters to describe the DCB and z-pinning.

$h$ (mm)	$w$ (mm)	$L$ (mm)	$a_0$ (mm)	$a_p$ (mm)	$\delta_a$ (mm)	$P_a$ (N)	$n_c$	$n_r$	$d_c$ (mm)
1.5	20	150	50	5	0.1	15	8	5	3.5